# 2

# Some-Long-Run Properties of Geophysical Records

B. B. Mandelbrot and J. R. Wallis

## PRESENTATION

By preparing this book Chris Barton and Paul La Pointe have earned the gratitude of all geologists and students of fractals. I continue to belong to this second group, and Chris and Paul clearly have put me in a very special debt to them.

How to express my thanks? They have suggested that I contribute a chapter to their book, an idea I found flattering but perhaps not completely appropriate. It would have been a great opportunity to write about long-run dependence and the statistical technique of *R/S* analysis, a topic that has fascinated me since around 1970, wide attention was drawn to it by Feder (1988). Historically the acceptance of long-run dependence had been an essential step toward formulating fractal geometry (Mandelbrot, 1982), and it has also helped give birth to an active branch of pure probability theory (Eberlein and Taqqu, 1986). From the scientists' viewpoint however, this specific chapter of fractal geometry was eventually submerged in a more general theory. As a result, it cries out for a fresh treatment.

In any event, I did not find the time to write a chapter. As an alternative, we all agreed that this book should reproduce a slightly edited version of a work that James R. Wallis and I published in *Water Resources Research*. This text may have escaped the attention of the broader community of geologists. In the process of reprinting, a few selected references later than 1969 have been added, and the bottom portions of all illustrations of *R/S* have been removed to take account of remarks in Taqqu (1970).

The original *Water Resources Research* paper was part of a series in that journal by the same authors, or by me alone, all of which are recommended to the reader. Abstracts of other papers in that series are appended to the present reprint (each followed by errata).

B. B. Mandelbrot

*B. B. Mandelbrot* • Yale University, New Haven, Connecticut, and IBM T. J. Watson Research Center, Yorktown Heights, New York. *J. R. Wallis* • IBM T. J. Watson Research Center, Yorktown Heights, New York.

*Fractals in the Earth Sciences*, edited by Christopher C. Barton and Paul R. La Pointe. Plenum Press, New York, 1995.

## 2.1. INTRODUCTION

Chapter 2 presents and comments on some long-run properties of geophysical records and in particular tests the validity of an empirical law Harold Edwin Hurst discovered during his preliminary studies for the future Aswan High dam (Hurst, 1951, 1956; Hurst and others, 1965). We show that this law must be amended, tightened, and hedged, but its essential claim is confirmed.

Hurst's law concerns the dependence of the rescaled bridge range on the lag $\delta$. It claims that $R(t,\delta)/S(t,\delta)$ takes the form $F\delta^H$, where $F$ is a prefactor and the exponent $H$ is constant, typically differing from 0.5. In this expression, $R(t,\delta)$ is the range of variation between the minimum and maximum values as a function of a particular starting time $t$ and lag $\delta$, while $S(t,\delta)$ is the standard deviation over the same $t$ and $\delta$.

Table 2.1 shows that in most cases $H \neq 0.5$. This inequality has striking consequences. If the records in question were generated by a random process such that observations far removed in time can be considered independent, $R(t,\delta)/S(t,\delta)$ would become asymptotically proportional to $\delta^{0.5}$. This means that Hurst's law would have to "break" for sufficiently large lags, but no such break has ever been observed. According to Mandelbrot and Wallis (1968), and the last section of Chapter 2, it follows that for all practical purposes, geophysical records must be considered to have an infinite span of statistical interdependence.

Fractional Gaussian noises discussed in Mandelbrot and Van Ness (1968) and Mandelbrot and Wallis (1969a), are a family of random processes specifically designed to satisfy Hurst's law. Comparing figures in Chapter 2 with those of Mandelbrot and Wallis (1969a) confirm in our opinion that geophysical records can be modeled by fractional noises. Analysis techniques are not discussed at length because they are found in Mandelbrot and Wallis (1969a), which the interested reader can consult. Definitions relative to spectra, being standard, are not repeated here; however the method of constructing the ratio $R/S$ and pox diagram notion are described in detail.

Extreme caution is required when using $R/S$ to analyze records where strong cycles are present. This circumstance is documented later, in particular in the case of sunspot numbers. As a result, $R/S$ may not be the most suitable statistic when strong cycles are present. The marginal distribution of the record on the contrary has little effect on the behavior of $R/S$.

The records studied in Chapter 2 fall into three subject matter categories:

Recent hydrological records of streamflow, rainfall, and temperature measurements; the longest among such records are records of annual maximum and minimum stage for the Nile River.

Fossil hydrological records, such as tree ring indices, varve thickness, and other records of geological deposits; the importance of such records in hydrology are discussed in the last section of Chapter 2.

Other miscellaneous records, such as sunspot numbers, earthquake frequencies, and directions of river meanders.

Figures in Chapter 2 represent a small fraction of our present files. We have withheld many figures that would be purely repetitive and a few that require extensive discussion. The remainder of Chapter 2 is devoted to a table of rough estimates of the H-coefficient (the basic parameter of Hurst's law) and to a text devoted to three subjects: the graphical devices

TABLE 2.1. Values of $H$ and of the Third and Fourth Moments for Some Geophysical Data[a]

| Description | $H$ | Moments | |
|---|---|---|---|
| | | Third | Fourth |
| **Varve Data from De Geer (1940) Swedish Time Scale** | | | |
| Haileybury, Canada, +310 to −369 | 0.80 | 0.74 | 4.41 |
| Timiskaming, Canada, +1321 to −588 | 0.96 | 1.03 | 6.33 |
| Sirapsbacken, Sweden, +576 to +257 | ≈1.00 | 0.95 | 3.52 |
| Degeron, Sweden, +499 to 0 | 0.97 | 1.10 | 3.65 |
| Omnas, Sweden, +1399 to +1162 | 0.65 | 3.39 | 23.01 |
| Resele, Sweden, +1399 to +1132 | 0.67 | 4.00 | 26.02 |
| Hammerstrand, Sweden, +2000 to +1767 | 0.85 | 2.10 | 9.04 |
| Ragunda, Sweden, +1933 to +1800 | 0.99 | 1.59 | 5.21 |
| Lago Corintos, Argentina, −801 to −1168 | 0.89 | 0.85 | 3.58 |
| Biano, Himalaya Mountains, −1180 to −1279 | 0.50 | 1.84 | 7.82 |
| Sesko, Himalaya Mountains, −1293 to −1374 | 0.99 | 0.31 | 2.20 |
| Enderit River, E. Africa, −406 to −546 | 0.91 | 1.07 | 4.10 |
| **Schulman (1956) Tree ring indices** | | | |
| Table 28, Douglas Fir and Ponderosa Pine, Fraser River, British Columbia, 1420–1944 | 0.70 | 0.19 | 2.84 |
| Table 30, Douglas Fir, Jasper, Alberta. 1537–1948 | 0.75 | 0.60 | 3.34 |
| Table 31, Douglas Fir, Banff, Alberta, 1460–1950 | 0.65 | 0.32 | 2.76 |
| Table 33, Douglas Fir and Ponderosa Pine, Middle Columbia River Basin, 1650–1942 | 0.75 | 0.10 | 3.20 |
| Table 36, Douglas Fir, Snake River Basin, 1282–1950 | 0.77 | 0.24 | 3.60 |
| Table 38, Limber Pine, Snake River Basin. 1550–1951 | 0.60 | −0.06 | 3.47 |
| Table 40, Douglas Fir, Upper Missouri River Basin, 1175–1950 | ≈0.50 | 0.33 | 3.14 |
| Table 41, Limber Pine, Upper Missouri River Basin, 978–1950 | 0.63 | 0.29 | 3.71 |
| Table 43, Douglas Fir, North Platte River Basin, 1336–1946 | 0.70 | 0.65 | 3.88 |
| Table 44, Douglas Fir, South Platte River Basin, 1425–1944 | 0.62 | 0.21 | 2.77 |
| Table 45, Douglas Fir, Arkansas River Basin, 1427–1950 | 0.66 | 0.03 | 2.86 |

(*Continued*)

TABLE 2.1. (*Continued*)

| Description | | Moments | |
|---|---|---|---|
| | *H* | Third | Fourth |
| Table 49, Mixed Species, three-year means, Colorado River Basin, 70 B.C. to 1949 A.D. | 0.55 | 0.25 | 3.07 |
| Table 50, Douglas Fir, Colorado River Basin, 1450–1950 | 0.64 | −0.15 | 2.82 |
| Table 52, Pinyon Pine, Colorado River Basin, 1320–1948 | 0.68 | −0.43 | 3.32 |
| Table 65, Ponderosa Pine, Upper Gila River, 1603–1930 | 0.69 | −0.07 | 3.25 |
| Table 66, Douglas Fir, Southern Arizona, 1414–1950 | 0.69 | −0.03 | 3.11 |
| Table 70, Douglas Fir, Upper Rio Grande, 1375–1951 | 0.65 | 0.21 | 2.88 |
| Table 71, Pinyon Pine, Upper Rio Grande, 1356–1951 | 0.68 | −0.23 | 2.76 |
| Table 72, Douglas Fir, Middle Rio Grande (Guadalupe), 1650–1941 | 0.59 | 0.24 | 2.87 |
| Table 73, Douglas Fir, Middle Rio Grande (Big Bend), 1645–1945 | 0.71 | 0.59 | 3.13 |
| Table 75, Ponderosa Pine, southeastern Oregon, 1453–1931 | 0.58 | 0.04 | 3.27 |
| Table 76, Ponderosa Pine, northeastern California, 1485–1931 | 0.78 | 0.11 | 3.12 |
| Table 77, Jeffrey Pine, east central California, 1353–1941 | 0.72 | −0.15 | 2.93 |
| Table 78, Big-cone Spruce, southern California, 1385–1950 | 0.56 | 0.11 | 3.62 |
| Table 79, Ponderosa Pine, southern California, 1350–1931 | 0.72 | −0.40 | 2.89 |
| Table 80, Douglas Fir, west central Mexico, 1640–1943 | 0.86 | −0.10 | 2.40 |
| Table 85, Cipres at Cerro Leon, Argentina, 1572–1949 | 0.91 | 0.41 | 3.41 |
| **Data from Statistical History of the United States (1965)** | | | |
| Annual Precipitation | | | |
| Albany, New York, 1826–1962 | 0.87 | 0.56 | 3.46 |
| Baltimore, Maryland, 1817–1962 | 0.75 | −0.06 | 2.64 |
| Charleston, South Carolina, 1832–1962 | 0.89 | 0.65 | 3.53 |
| New Haven, Connecticut, 1873–1962 | 0.73 | 0.30 | 2.33 |
| New York, New York, 1826–1962 | 0.65 | 0.59 | 2.89 |
| Philadelphia, Pennsylvania, 1820–1962 | 0.81 | 0.21 | 2.85 |
| San Francisco, California, 1850–1963 | 0.64 | 0.45 | 3.11 |
| St. Louis, Missouri, 1857–1962 | 0.64 | 0.63 | 4.20 |
| St. Paul, Minnesota, 1837–1962 | 0.67 | 0.49 | 5.15 |
| **Data from Ruth B. Simon (Personal Communication)** | | | |
| Weekly derby earthquake frequencies, April 1962–June 1967 | 0.93 | 3.99 | 24.45 |

(*Continued*)

TABLE 2.1. (*Continued*)

| Description | | | Moments | |
|---|---|---|---|---|
| | | *H* | Third | Fourth |
| **Munro (1948) Sunspot data (1749–1948)** | | | | |
| Monthly sunspot frequency 1749–1948 | | 0.96 | 1.04 | 3.88 |
| **Data from V.M. Yevdjevich (1963)** | | | | |
| Gota River near Sjotrop-Vanersburg, Sweden, 1807–1957 | $U^b$ | ≈0.50 | −0.06 | 2.35 |
| | $Y^c$ | ≈0.50 | 0.42 | 2.94 |
| Neumunas River at Smalininkai, Lithuania, 1811–1943 | $U^b$ | 0.61 | 0.47 | 3.15 |
| | $Y^c$ | 0.48 | 0.61 | 3.31 |
| Rhine River near Basle, Switzerland, 1807–1957 | $U^b$ | ≈0.50 | 0.14 | 2.80 |
| | $Y^c$ | ≈0.50 | 0.23 | 2.89 |
| Danube River at Orshawa, Romania, 1837–1957 | $U^b$ | ≈0.50 | 0.27 | 2.26 |
| | $Y^c$ | ≈0.50 | 0.22 | 2.53 |
| Mississippi River near St. Louis, Missouri, 1861–1957 | $U^b$ | 0.79 | 0.29 | 2.75 |
| | $Y^c$ | 0.68 | 0.18 | 2.45 |
| St. Lawrence River near Ogdensburg, New York, 1860–1957 | $U^b$ | 0.98 | −0.26 | 2.70 |
| | $Y^c$ | 0.69 | 0.14 | 2.70 |
| **Professor J. C. Mann, Data from Paleozoic Era Sediments (Personal Communication)** | | | | |
| Wolfcampian Section, Kansas | Thickness of beds | 0.75 | 4.60 | 32.27 |
| | Lithology of beds | 0.71 | 0.25 | 2.97 |
| Virginian–Desmoinesian Section, Superior, Arizona | Lithology of beds | 0.55 | 0.78 | 3.27 |
| | Bedding type | 0.67 | 0.19 | 2.21 |
| Missourian–Atokan Section, Honacker Trail, Utah | Thickness of beds | 0.70 | 3.51 | 24.81 |
| | Lithology of beds | 0.61 | −0.05 | 2.06 |
| | Bedding type | 0.58 | 0.47 | 2.11 |
| **Data from J. de Beauregard (1968)** | | | | |
| Rhine River, monthly flows, 1808–1966 | | 0.55 | 0.65 | 3.01 |
| Loire River, monthly flows, 1863–1966 | | 0.69 | 1.53 | 5.47 |
| **Nile River Data, Prince Omar Toussoun (1925)** | | | | |
| Annual maximums, 622–1469 | | 0.84 | −0.86 | 7.04 |
| Annual minimums, 622–1469 | | 0.91 | 0.32 | 3.50 |
| **Data from J. G. Speight (Personal Communication)** | | | | |
| Moorabool River meander azimuths | | 0.73 | 0.07 | 2.82 |

[a]The first and second moments were, in all cases, normalized to be 0 and 1, respectively.
[b]Unadjusted for overyear carryover.
[c]Adjusted for overyear carryover.

we call pox diagrams, pitfalls in the statistical estimation of H, and the significance of Hurst's findings in geophysics.

## 2.2. *R/S* AND POX DIAGRAMS

The following definition of the rescaled bridge range for an empirical record parallels the definition of the rescaled bridge range for a random process as given in Mandelbrot and Wallis (1969a).

Let $X(t)$ be a record containing $T$ readings uniformly spaced in time from $t = 1$ to $t = T$, and let $\int X(t)$ designate $\Sigma_{u=1}^{t} X(u)$. Thus

$$\delta^{-1} \int X(\delta)$$

is the average of the first $\delta$ readings, and

$$\delta^{-1}[\int X(t + \delta) - \int X(t)]$$

is the average of readings within the subrecord from time $t + 1$ to time $t + \delta$.

The $S^2(t,\delta)$ is defined as the sample variance of the subrecord from time $t + 1$ to $t + \delta$, namely,

$$S^2(t,\delta) = \delta^{-1} \sum_{u=t+1}^{t+\delta} X^2(u) - \left[\delta^{-1} \sum_{u=t+1}^{t+\delta} X(u)\right]^2 \tag{1}$$

The bridge range $R(t,\delta)$, illustrated in Fig. 2.1, is defined as follows

$$\begin{aligned} R(t,\delta) = &\max_{0 \leq u \leq \delta} \{\int X(t + u) - \int X(t) - (u/\delta)[\int X(t + \delta) - \int X(t)]\} \\ &-\min_{0 \leq u \leq \delta} \{\int X(t + u) - \int X(t) - (u/\delta)[\int X(t + \delta) - \int X(t)]\} \end{aligned} \tag{2}$$

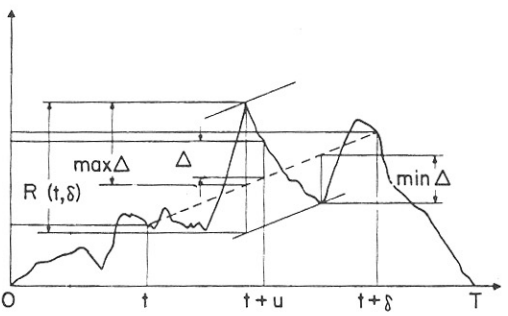


FIGURE 2.1. Construction of the sample bridge range $R(t,\delta)$ for a given sequence $X(t)$. To make the graph more compact and more legible, we have plotted (*bold line*), the bridge function of the whole sample, defined as $\Delta(t,0,T) = \int X(t) - (t/T)\int X(T)$. Replacing $\int X(t)$ with $\Delta(t,0,T)$ does not affect the values of $\Delta(u)$ or $R(t,\delta)$, two quantities defined below. Moreover, since empirical records are necessarily taken in discrete time, the function $\Delta$ should have been drawn as a series of points, but it was drawn as a line for the sake of clarity. The bridge function of the sample from $t + 1$ to $t + \delta$ is defined as

$$\Delta(u,t,\delta) = \int X(t + u) - \int X(t) - (u/\delta)[\int X(t + \delta) - \int X(t)]$$

and denoted by $\Delta$ in Fig. 2.1. The sample bridge range is defined as

$$R(t,\delta) = \max_{0 \leq u \leq \delta} \Delta(u,t,\delta) - \min_{0 \leq u \leq \delta} \Delta(u,t,\delta)$$

The ratio $R(t,\delta)/S(t,\delta)$ is then called a rescaled bridge range. Given the lag $\delta$, the starting $t$ could assume $T - \delta + 1$ different values, but the resulting mass of values of $R(t,\delta)/S(t,\delta)$ is both redundant and unmanageable. The data were replaced by averages, but the resulting reduction was in our opinion too drastic. The middle ground we chose is to plot the values of $R(t,\delta)/S(t,\delta)$ in the form of what we call a pox diagram.

To construct a pox diagram, we select a limited sequence of equally spaced values for $\log \delta$ and marked these on the horizontal axis of double logarithmic paper. For each $\delta$, we select a limited number of starting points $t$, then plot on the vertical axis the corresponding values of $R(t,\delta)/S(t,\delta)$ so obtained. Thus above every marked value of $\delta$, several points (enlarged into + signs) are aligned. For each $\delta$, the sample average of the quantities $R(t,\delta)/S(t,\delta)$ is marked by a little square box. The line connecting the boxes weaves through the pox diagram.

*The trend line of the pox diagram and Hurst's law.* An empirical record is said to satisfy Hurst's law if, except perhaps for very small and very large values of $\delta$, the pox diagram of $R(t,\delta)/S(t,\delta)$ is tightly aligned along a straight trendline whose slope is designated by $H$. Originally Mandelbrot (1965) chose the letter $H$ to honor Hurst, but since the 1970s and 1980s, $H$ is often related to the Hölder exponent. Theory shows that in all cases, $0 < H < 1$, and in geophysics $H > \frac{1}{2}$. The value $H = 0.5$ has a special significance because it suggests that observations sufficiently distant from each other in time are statistically independent.

Mandelbrot and Wallis (1969b) discuss the concepts of tight alignment along a trend line more precisely and define several variants (of increasingly demanding scope) of the $\delta^H$ law.

## 2.3. PITFALLS IN THE GRAPHIC ESTIMATION OF $H$

Until better estimation procedures are developed, the exponent $H$ must be estimated graphically from something like the pox diagram. The following pitfalls in this approach exist.

### *2.3.1. The Initial Transient*

For small values of $\delta$, the scatter of the values of $R(t,\delta)/S(t,\delta)$ is large, and various irrelevant influences are felt. Consequently even if values of $R/S$ for small $\delta$ are known, they should be disregarded when drawing conclusions from the pox diagram.

### *2.3.2. The Final Tightening of the Pox Diagram*

Let the total sample run from $t = 1$ to $t = T$. For small $\delta$, the starting points t can be so selected that the corresponding subsamples from $t + 1$ to $t + \delta$ remain nonoverlapping, whereas the number of subsamples remains large. For larger $\delta$, the situation is not so ideal. We have the choice between very few nonoverlapping subsamples and a larger number of overlapping subsamples. Either choice narrows the pox diagram; the former does so because few points are strongly correlated and differ little from each other.

### *2.3.3. Graphically Fitting a Straight Trend Line*

The fact that pox diagrams exhibit an initial transient and final tightening implies that when fitting a straight trend line, small and large values of $\delta$ should be given less weight than values removed from both $t = 1$ and $\delta = T$.

### 2.3.4. *A Warning against an Error in Hurst's Initial Statement of His Law*

The statement we call Hurst's law is a significant innovation. Hurst (1951) claimed that the pox diagram of $R/S$ has a trend line going through the point of abscissa $\log 2$ and the ordinate $\log 1 = 0$, which means that Hurst took the prefactor and the exponent to be related by $F = 2^{-H}$. Hurst's claims led to the following estimation procedure: In cases where $R(t,\delta)/S(t,\delta)$ was known for a single sample from $t + 1$ to $t + \delta$, he estimated $H$ to be

$$K(t,\delta) = \frac{\log [R(t,\delta)/S(t,\delta)]}{\log \delta - \log 2} \tag{3}$$

In cases where $R(t,\delta)/S(t,\delta)$ was known for more than one sample, he averaged the values of the function $K(t,\delta)$ corresponding to all the points of coordinates of $\delta$ and $R/S$.

Actual pox diagrams have a straight trend line of slope $H$ that fails to pass through the point of abscissa $\log 2$ and ordinate 0. Hurst's average $K$ is thus a very poor estimate of the slope $H$: It tends to be too low when $H > 0.72$ and too high when $H < 0.72$. As a result, the trend line and Hurst's method may both suggest identical typical values for $H$, but Hurst's method greatly underestimates the variability of $H$ around its typical value. The reader can verify the preceding statements in Figs. 2–7 of Mandelbrot and Wallis (1969a, part 2). For such processes as the stuttering noises of Mandelbrot and Wallis (1969b), the results of Hurst's method are entirely meaningless. To avoid confusion, we labeled the actual slope with the letter $H$, which differs from the letter $K$ used by Hurst.

## 2.4. DETERMINING $H$ FOR A SPECIFIC HYDROLOGICAL PROJECT

We found great variability in the values of $H$ measured on $R/S$ pox diagrams of actual records. To explain such variability may prove difficult. When designing a specific hydrological project, we must in many cases be content with an intelligent but imprecise estimated value of $H$. When data needed to determine $H$ for a certain river are unavailable, related hydrological records may be usable. Regardless of the data used, $H$ is far from 0.5, except for such obviously well-behaved rivers as the Rhine, which is analyzed in Fig. 2.9. However the difficulty of estimating $H$ is an extremely poor justification for an indiscriminate use of short-memory models that imply that $H = 0.5$.

### 2.4.1. *A Warning Concerning Sunspot Records and Other Cases with a Strong Periodic Element*

To see the effect of strong periodic elements on a pox diagram of $R/S$, examine Fig. 2.2 relative to the Wolf sunspot numbers; also examine Fig. 2.3, which enlarges the portion of Fig. 2.2 near a lag of $\delta = 11$ years $= 132$ months, the wavelength of the well-known periodic element in sunspot numbers. We clearly see (1) a contraction in the scatter of the values of $\log [R(t,\delta)/S(t,\delta)]$ and (2) a break in the trend line, shaped like a horizontally laid reverse $S$. The partial trend lines before and after the 11-year break have equal slopes, with H much exceeding 0.5.

The contraction and break are both characteristic consequences of the presence of a strong periodic element. In addition, we observe other breaks, corresponding to each subharmonic of $\delta = 11$ years. Since however $H$ is very large in the sunspot case, the other

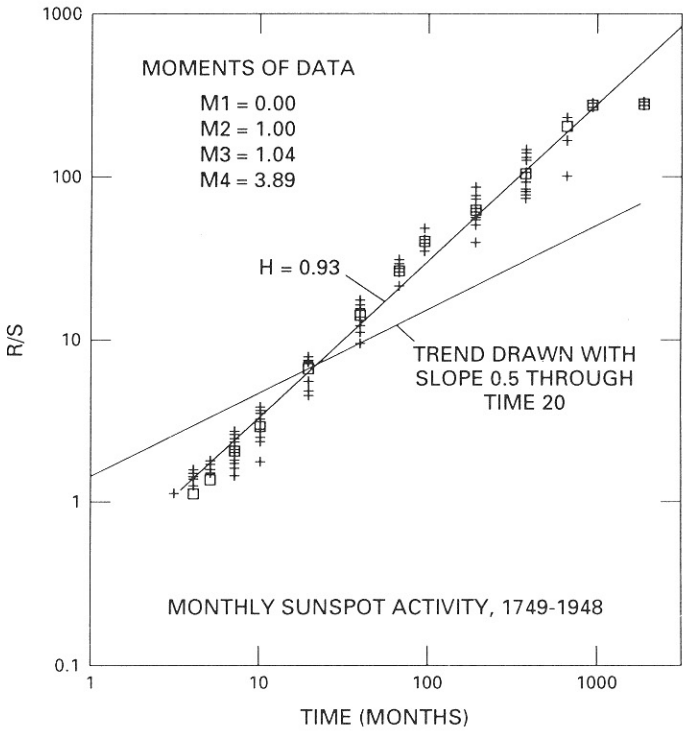


FIGURE 2.2. Pox diagram of $\log R/S$ versus $\log \delta$ for the monthly Wolf numbers of sunspot activity, as reported by Munro (1948) (skewness = 1.04; kurtosis = 3.89). In this and later figures relative to $R/S$, time means time lag. In Fig. 2.2, the slope of the trend line greatly exceeds 0.5. This new observation is much more apparent than the well-known presence in sunspot numbers of a cycle of 11 years = 132 months and perhaps of a cycle of 80 years. Each of these cycles manifests itself mainly by a narrowing of the pox diagram followed by a break shaped like a horizontally laid letter S. Before drawing any conclusion from the high apparent value of H for sunspots, the reader should consult Mandelbrot and Wallis (1969b).

This pox diagram was constructed as follows: Dots (+) correspond to values of the lag $\delta$ restricted to the sequence 3, 4, 5, 7, 10, 20, 40, 70, 100, 200, 400, 700, 1000, 2000, 4000, 7000, and 9000. For every $\delta$ satisfying $\delta < 500$, we plot 14 dots, corresponding to values of t equal to 1, 100, . . . , 1400. For every $\delta$ satisfying $\delta > 500$, t was made successively equal to 1000, 2000, up to either 8000 or $(T - \delta) + 1$, whichever is smaller.

breaks are weak. Hence the presence of a periodic element complicates the picture, but it does not hide the Hurst phenomenon. Note also that the 80-year cycle reported by Willett (1964), which does not appear on the spectral pox diagram of the sunspot data (see Fig. 2.4), has been detected at the extremity of Fig. 2.2.

In other examples, the basic one-year cycle and its subharmonics overwhelm the long-run interdependence expressed by Hurst's law, and the value of $H$ cannot be inferred graphically from the pox diagram of $R/S$ built with raw data. The presence of several periodic elements of different wavelengths makes the situation even more complicated. For example, let several cyclic components be added to a fractional noise with a medium-sized value of $H$. The breaks corresponding to each period and its subharmonics merge together and yield a pox diagram with a much reduced apparent slope. The slope may fall below 0.5, and the diagram may even appear horizontal. For enormous values of $\delta$, a trend line of slope

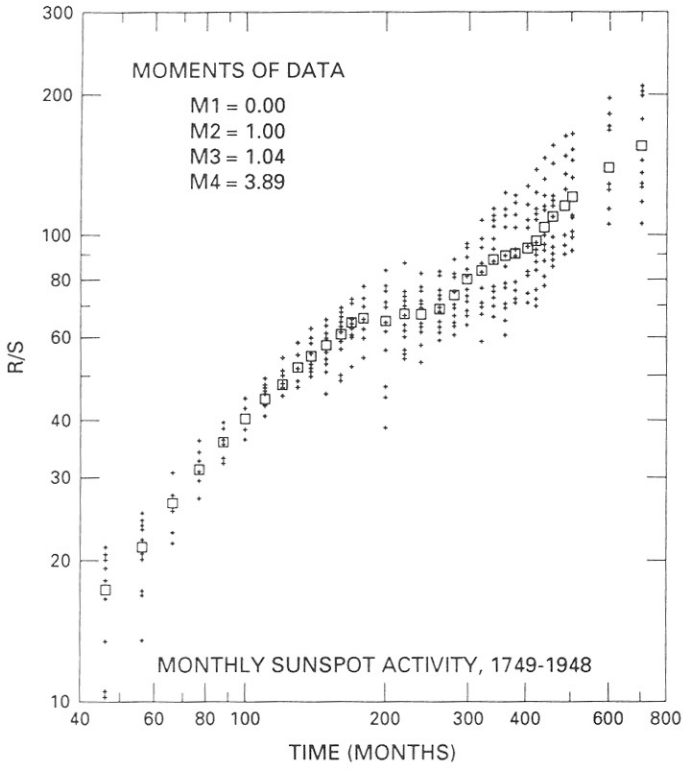


FIGURE 2.3. Detail of portion of Fig. 2.2. The preceding caption describes how we observed, near the lag corresponding to the 11-year cycle (132 month) cycle, a narrowing followed by break, which is characteristic of strongly cyclic phenomena. It was imperative to blow up this narrowing to examine details. In the resulting pox diagram, values of $\delta$ range from 50–180, uniformly spaced by increments of 10, then from 180–500 uniformly spaced by increments of 20, with two additional values at 600 and 700. For each $\delta$, values of $t$ were uniformly spaced with increments of 159. Several breaks are clearly visible here.

$H$ ultimately reestablishes itself, but as we have argued in many other contexts, an asymptotic behavior is of little use either in engineering or science unless it is very rapidly attained. Examples where strong subharmonics coexist with multiple cycles require lengthy discussion, and these are not presented in Chapter 2.

In summary, the pox diagrams of $R/S$ are less useful in the presence of strong periodic elements. Fortunately most periodic elements in natural records are fairly obvious, and these can be removed; the search for hidden periodicities is usually fruitless. In the following section, draw $R/S$ pox diagrams of the corrected records remaining after periodic elements are removed.

No clear cut cyclic effect is present in data analyzed in Figs. 2.5–2.16.

### 2.4.2. *Significance of Hurst's Law in Geophysics*

Among the classical dicta of the philosophy of science is Descartes's prescription "to divide every difficulty into portions that are easier to tackle than the whole." This advice

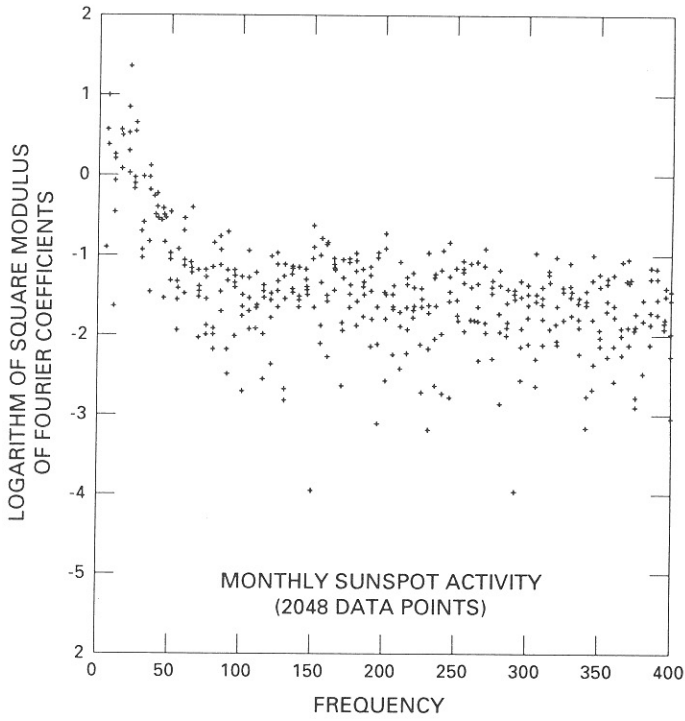


FIGURE 2.4. Pox diagram of the Fourier coefficients of sunspot activity. The total sample was reduced to 2048 pieces of data to enable us to use a Fast Fourier Transform computer program. The frequency is measured in number of cycles per 2048 pieces of data. Frequencies are grouped together in fives, with the $h$th group made of the frequencies $5h$, $5h$ --1, $5h$ --2, $5h$ --3, and $5h$ --4, where $h$ takes all positive integer values. Values of the squared Fourier moduli corresponding to frequencies in a group are all plotted above the abscissa, corresponding to the highest frequency in such a group, namely, $5h$. This procedure introduces a local smoothing that eliminates many apparent cycles and makes it possible to some extent to avoid spectral window processing of Fourier coefficients (see Mandelbrot and Wallis, 1969a, part 2). Curiously the well-known 11-year period of sunspot numbers does not appear as a sharp peak in Fourier coefficients but continues the tendency of the diagram to rise sharply as k decreases. Using spectral windows on the same data, as in Granger and Hatanaka (1964, p. 66), leads to essentially the same conclusion reached by this pox diagram.

has been extraordinarily useful in classical physics, because boundaries between distinct subfields of physics are not arbitrary. They are intrinsic in the sense that phenomena in different fields interfere little with each other and each field can be studied alone before a description of the mutual interactions is attempted.

Subdivision into fields is also practiced outside of classical physics. Consider, for example, atmospheric science. Students of turbulence examine fluctuations with time scales of the order of seconds or minutes; meterologists concentrate on days or weeks; specialists whom we may call macrometerologists concentrate on periods of a few years; climatologists deal with centuries; and finally paleoclimatologists are left to deal with all longer time scales. The science that supports hydrological engineering falls somewhere between macrometerology and climatology.

The question then arises whether or not this division of labor is intrinsic to the subject

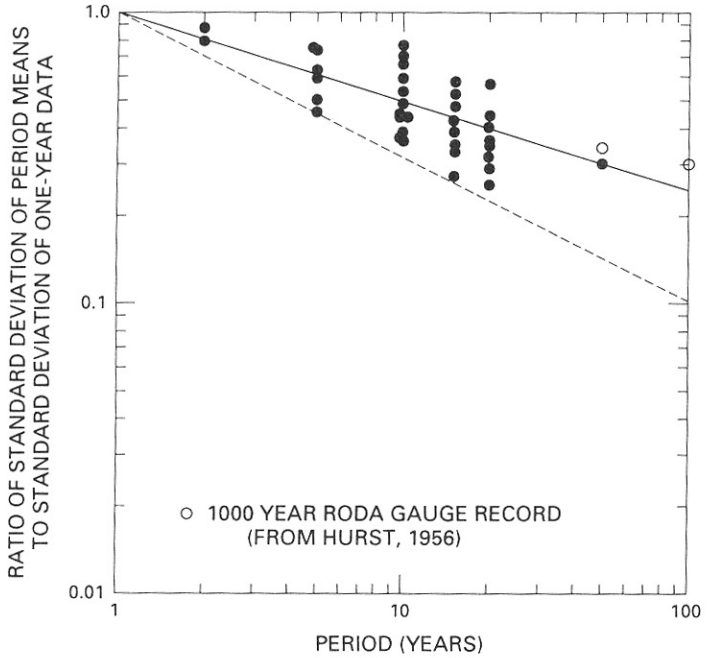


FIGURE 2.5. A superposition of several variance–time diagrams. To draw the variance–time diagram of a record, select a sequence of lags $\delta$ (plotted as abscissas). For each $\delta$, average $\delta$ successive pieces of data in a record, then compute the variance of these $\delta$-year averages around the overall average of each sample. The quantity plotted on the ordinate is the ratio of this variance for $\delta$ plotted on the abscissa and $\delta = 1$. Several variance–time diagrams are superposed on Fig. 1.5, which does not represent new calculations but is reproduced with the author's permission from Langbien (1956), who used miscellaneous records from Hurst (1956). Superposition has eliminated much of the information in the data, and Fig. 1.5 shows only that every one of the superposed variance–time diagrams is located above the dashed line, which has slope $H - 0.5$. That line represents the behavior to be expected if observations placed at very distant instants of time were independent. The variance decreases less rapidly than expected because the $R/S$ pox diagram has a trendline of slope $H > 0.5$ and the Fourier pox diagram rises steeply for low frequencies. The last two points to the right are for Hurst's data concerning the 1000-year record of Rhoda gauge readings.

matter. In our opinion, it is not, in the sense that it does not seem possible when studying a field in the preceding list to neglect its interactions with others. We fear therefore that dividing the study of fluctuations into distinct fields is mainly a matter of convenient labeling, but it is hardly more meaningful than either classifying bits of rock into sand, pebbles, stones, and boulders or enclosed water-covered areas into puddles, ponds, lakes, and seas.

Take the example of macrometerology and climatology. Although they can be defined formally as the sciences of fluctuations on time scales respectively smaller and longer than one lifetime, macrometerology and climatology should not be considered as really distinct unless and until they have actually been shown to be ruled by processes that can be separated from each other by actual experiment. In particular, there should exist at least one duration $\lambda$ for a record, with $\lambda$ of the order of magnitude of one lifetime, that is both long enough for macrometerological fluctuations to be averaged out and short enough to keep

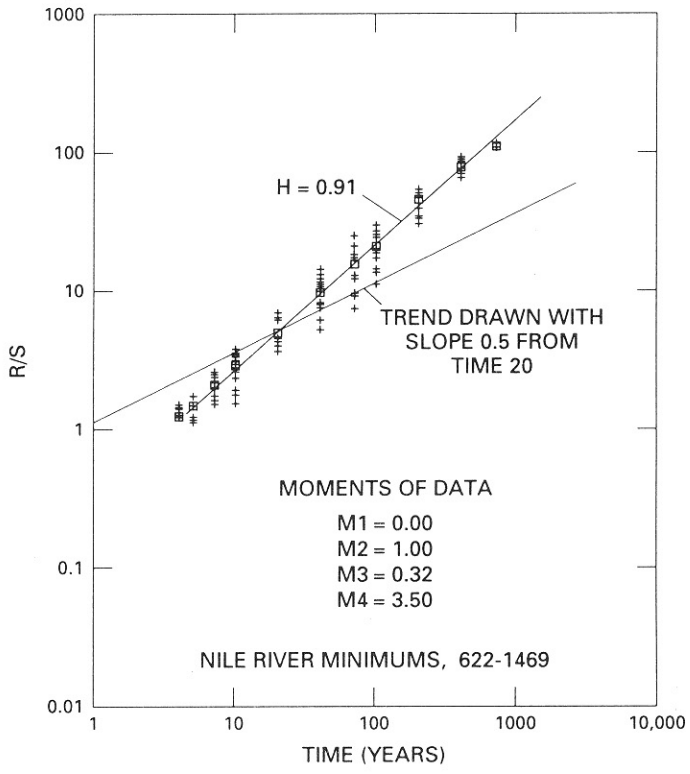


FIGURE 2.6. Pox diagram of $\log R/S$ versus $\log \delta$ for the Nile minimums, as reported in Toussoun (1925) (skewness = 0.32, kurtosis = 3.50). This pox diagram was constructed as in Fig. 2.2. The Nile is interesting for three reasons: It is the site of the biblical story of Joseph, which suggested to Mandelbrot and Wallis (1968) the term Joseph effect; it is the river whose flow Hurst's investigations were designed to help regularize; and it is the object of the longest available written hydrological records. The $R/S$ pox diagram of Nile maximums is not plotted because it is extremely similar to the diagram shown in Fig. 2.6.

clear of climate fluctuations. We examine how the existence of such a $\lambda$ would affect spectral analysis and $R/S$ analysis.

Unfortunately both spectral and $R/S$ analyses possess limited intuitive appeal. Let us therefore first discuss a more intuitive example of the kind of difficulty encountered when two fields gradually merge into each other. We summarize the discussion in Mandelbrot (1967a) of the concept of the length of a seacoast or a riverbank, see also Mandelbrot (1982). To measure a coast with increasing precision, start with a very rough scale and add increasingly finer detail. For example, walk a pair of dividers along a map and count the number of equal sides of length $G$ of an open polygon whose vertices lie on the coast. When $G$ is very large, the length is obviously underestimated. When $G$ is very small, the map is extremely precise; the approximate length $L(G)$ accounts for a wealth of high-frequency details that are surely outside the realm of geography. As $G$ is made very small, $L(G)$ becomes meaninglessly large. Now consider the sequence of approximate lengths corresponding to a sequence of decreasing values of $G$. The $L(G)$ may increase steadily as $G$ decreases, but the zones in which $L(G)$ increases may be separated by one or more

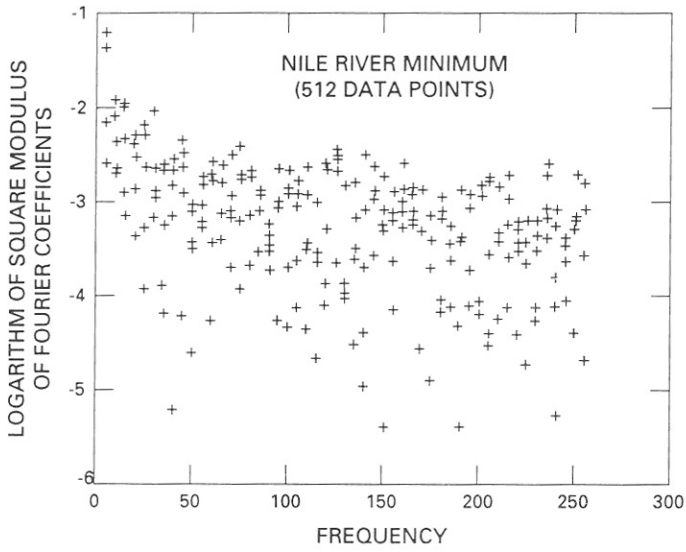


FIGURE 2.7. Spectral pox diagram of Nile minimums. The rise of the diagram, as $k$ decreases, confirms that the value of $H$ is large, as observed in fig. 2.6.

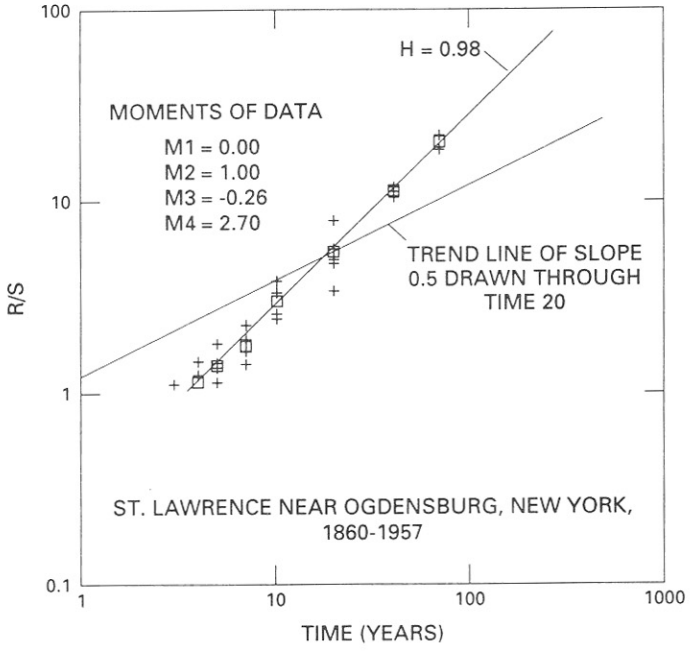


FIGURE 2.8. Pox diagram of $\log R/S$ versus $\log \delta$ for the annual flow of the St. Lawrence River. Data are from Yevjevich (1963) (skewness = $-0.26$, kurtosis = 2.7). This pox diagram was constructed as in Fig. 2.2. Note observed that the estimate of H in Table 2.1 would be substantially modified if carry over were taken into account.

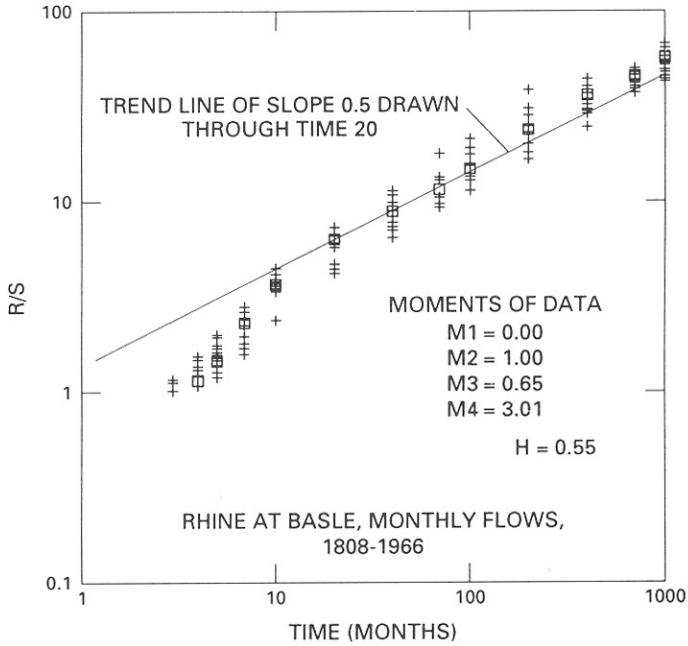


FIGURE 2.9. Pox diagram of $\log R/S$ versus $\log \delta$ for the annual flow of the Rhine River. Data are from de Beauregard (1968) (skewness = 0.65; kurtosis = 3.01). This pox diagram was constructed as follows: Log $\delta$ was restricted to the values 3, 4, 5, 7, 10, 20, 40, 70, 100, 200, 400, 700, 1000, 2000, 4000, 7000, and 9000. For every $\delta$, we selected 15 values of $\delta$, spaced uniformly over the available samples. The Rhine provides a rare example of river flow in which the asymptotic slope of the trend line is very nearly 0.5. This means that low-frequency effects equaling $H > 0.5$ are absent or weak and high-frequency effects are not overwhelmed. In our opinion, dealing with low-frequency effects (when present) takes precedence over dealing with high-frequency effects to which traditional statistical models are exclusively devoted. In the case of the Rhine, it appears legitimate to use models restricted to high-frequency effects.

"shelves" where $L(G)$ is essentially constant. To define clearly the realm of geography, we think it is necessary for a shelf to exist for values of $G$ near $\lambda$, where features of interest to the geographer satisfy $G \gg \lambda$ and geographically irrelevant wiggles satisfy $G \ll \lambda$. If a shelf exists, we can call $G(\lambda)$ a coast length. A shelf indeed has been observed for many coasts marked by sand dunes and also for many man-regulated coasts (say, the Thames in London). In many cases however, there is no shelf in the graph of $L(G)$, and the concept of length must be considered entirely arbitrary. Similar comments have been made in other contexts, such as the distinction between domains of relevances of economics and the theory of speculation in Mandelbrot (1963).

After this preliminary, let us return to the distinction between macrometerology and climatology. It can be shown that to make these fields distinct, the spectral density of the fluctuations must have a clear-cut dip in the region of wavelengths near $\lambda$, with large amounts of energy on both sides. This dip would be the spectral analysis counterpart of the shelf in coast length measurements. But in fact no clear-cut dip is ever observed.

Similarly from the viewpoint of $R/S$ analysis, macrometerology and climatology are not distinct sciences unless the pox diagram of $R/S$ exhibits distinct macrometerology and

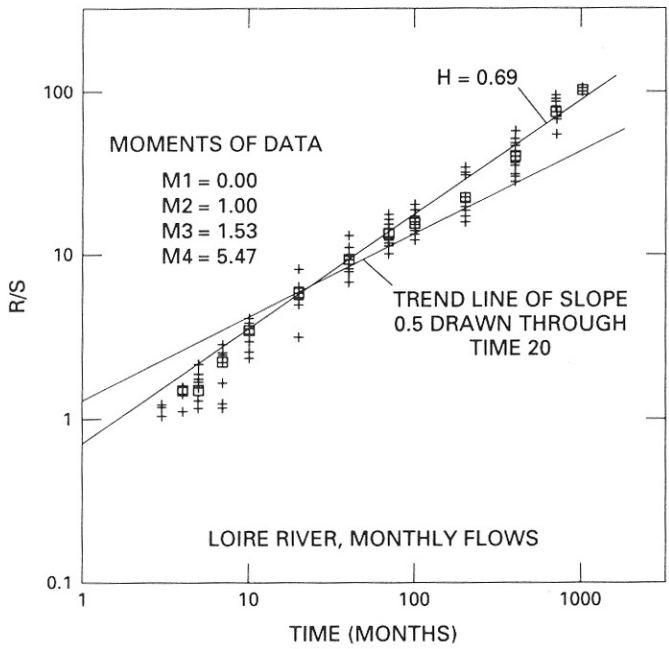


FIGURE 2.10. Pox diagram of $\log R/S$ versus $\log \delta$ for the annual flow of the Loire River. Data are from de Beauregard (1968) (skewness = 1.33, kurtosis = 5.47). This pox diagram was constructed as in Fig. 2.9. The fact that the value of $H$ is much larger for the Loire than for the Rhine fully confirms the intuitive feeling of French literary geographers about the respective degrees of irregularity of these two rivers. Whenever possible we should substitute the value of H for the geographer's intuitive descriptions. The latter may however be available in cases where the former is unattainable. To make such intuitive knowledge viable, it is useful to establish a correlation between $H$ and intuition in cases where both are available.

climatology regimes, with an intermediate regime near $\delta = \lambda$, where a variety of configurations is conceivable. To distinguish between macrometerology and climatology, the intermediate regime of the $R/S$ diagram must be clearly marked, with a straight trend line of slope 0.5; this region is the $R/S$ analysis counterpart of the shelf in coast length measurements. The narrower the separating regime, the less clear is the distinction between macrometerology and climatology. At the limit, our two fields cannot be distinguished unless the $R/S$ diagrams are very different for $\delta < \lambda$ and $\delta > \lambda$. For example, Hurst's law may apply for $\delta < \lambda$ with an exponent $H_1 \neq 0.5$ and for $\delta > \lambda$ with an exponent $H_2$ differing from both 0.5 and $H_1$.

When we wish to determine whether or not such distinct regimes are in fact observed, short hydrological records of 50 or 100 years are of little use. Much longer records are needed; thus, we followed Hurst in searching for very long records among the fossil weather data exemplified by varve thickness and tree ring indices. However even when the $R/S$ pox

FIGURE 2.12. Pox diagram of $\log R/S$ versus $\log \delta$ for a dendrochronological series from Schulman (1956) (skewness = 0.24, kurtosis = 3.60). Other records in Schulman yield extremely similar pox diagrams. However, measured values of $H$ vary greatly between different trees in the same general geographical area. This variability confirms that long-run characteristics of tree growth are highly sensitive to microclimatic circumstances.

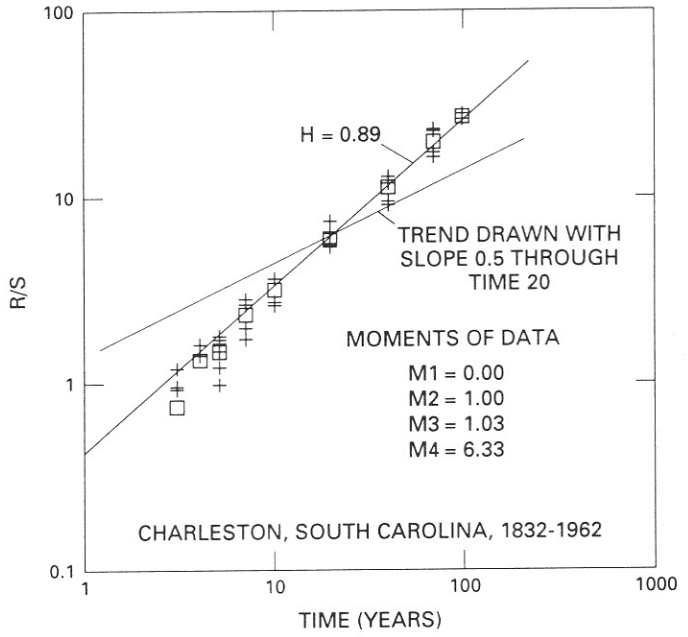


FIGURE 2.11. Pox diagram of $\log R/S$ versus $\log \delta$ for precipitation in Charleston, South Carolina. Data are from the US Bureau of the Census (1965) (skewness = 0.65, kurtosis = 3.5). Other precipitation records from the same source yield diagrams essentially indistinguishable from this example.

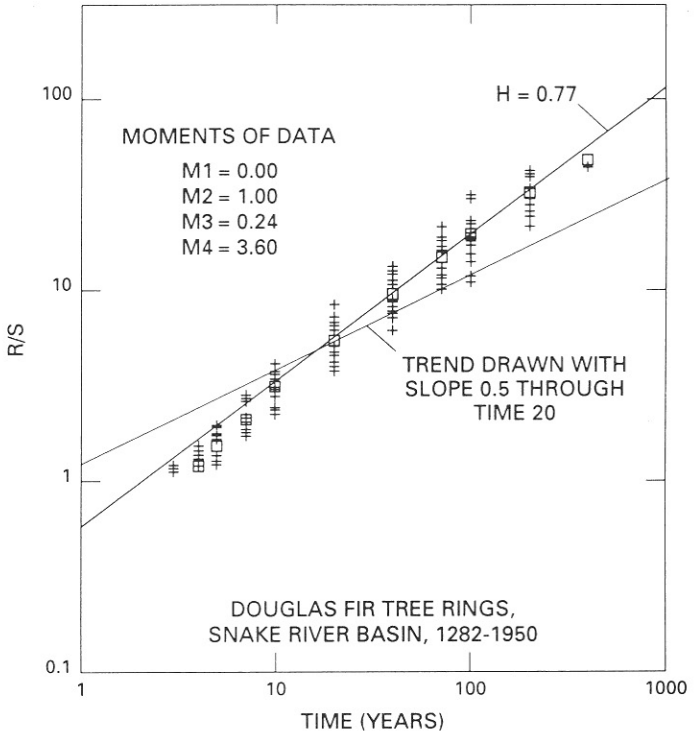

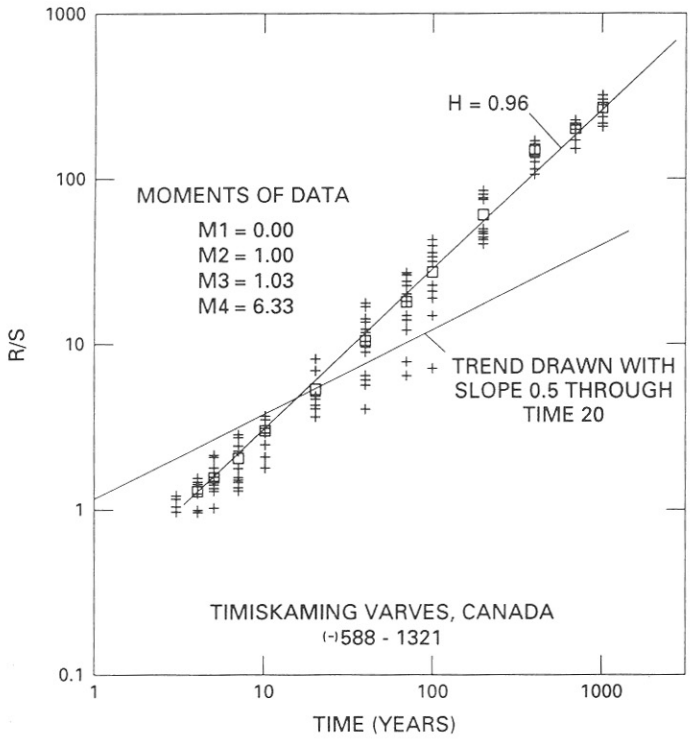


FIGURE 2.13. Pox diagram of $\log R/S$ versus $\log \delta$ for the thickness of varves in Timiskaming, Canada. Data are from De Geer (1940) (skewness = 1.03, kurtosis = 6.33). Other records in de Geer yield extremely similar pox diagrams. The present example was selected because its length is unusual even among varve records. Every time an unusually long record becomes available, we rush to check whether the slope of the $R/S$ pox diagram returns to the value of 0.5 corresponding to asymptotic independence. So far we are aware of no example of such a return. (Returns due to very strong cyclic effects are a different matter.)

diagrams are so extended, they still do not exhibit the kind of break that identifies two distinct fields.

We can now return to the claim made at the beginning of Chapter 2: The span of statistical interdependence of geophysical data is infinite. By this we mean only that this span is longer than the longest records so far examined. This gives to the term "infinity" a physical definition rather than the well-known mathematical definition (namely, "something" larger than any real number). For a detailed discussion of physical infinity, see Mandelbrot (1963). Among the related works that have been published since the original issue of Chapter 2, see Mandelbrot (1982).

In summary, even though distinctions between macrometerology and climatology or between climatology and paleoclimatology are unquestionably useful in ordinary discourse, they are not intrinsic to the subject matter, and it is imprudent to let them influence hydrological design.

One last word about why $H$ is so well-defined for so many geological data? Why is the Rhine well-behaved with $H = 0.5$, while the typical river yields $H > 0.5$? We can state the problem, but we have no solution to offer.

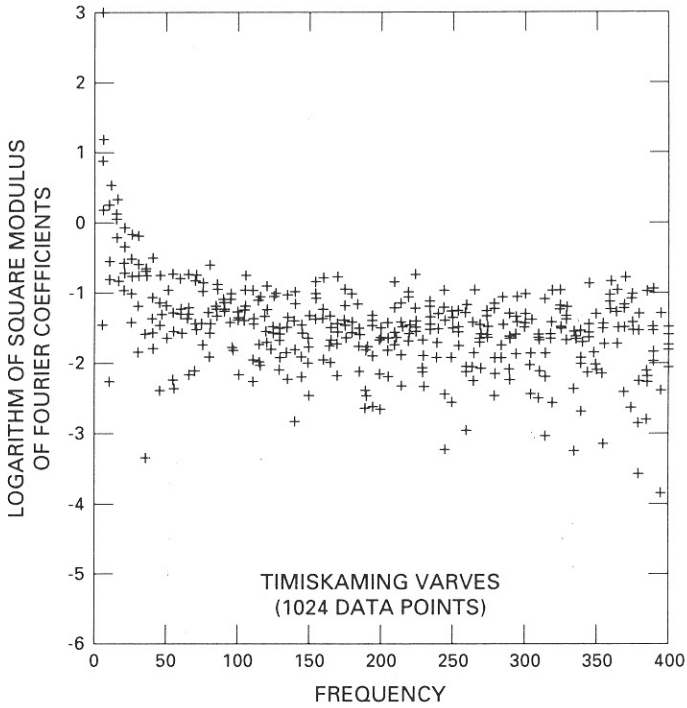


FIGURE 2.14. Fourier pox diagram from Timiskaming varves. Frequencies are plotted on a linear scale of the abscissas. The extremely steep low-frequency rise of this diagram confirms the high value of $H$ noted in Fig. 2.13.

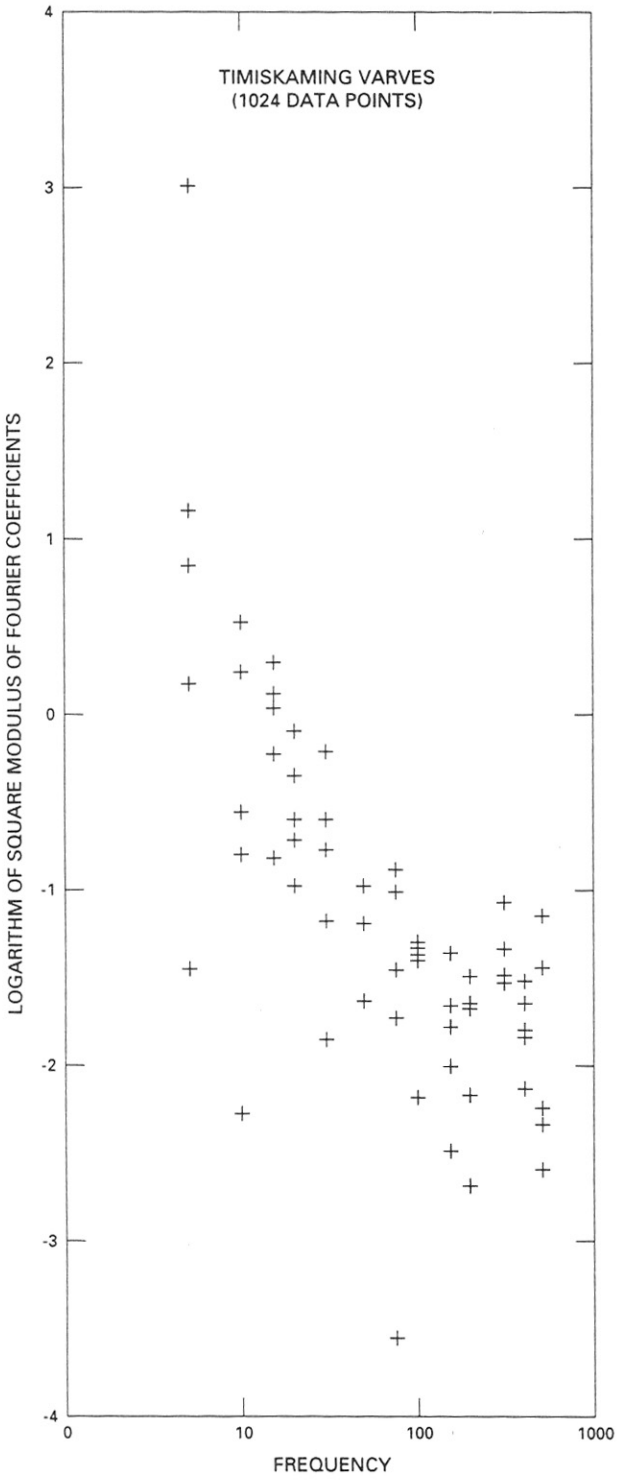


FIGURE 2.15. Alternative plot on double-logarithmic coordinates of the Fourier pox diagram for Timiskaming varves. For clarity only a small number of Fourier coefficients is plotted. Above the abscissa $k$, where $k$ is one of the frequencies 5, 10, 15, 20, 30, 75, 100, 150, 200, 300, 400, 500, 700, we plotted Fourier coefficients corresponding to the frequencies $k$, $k-1$, $k-2$, $k-3$, and $k-4$. There is some inconclusive evidence of a dip in spectral density in the neighborhood of frequency 200, corresponding to a wavelength of 5 years.

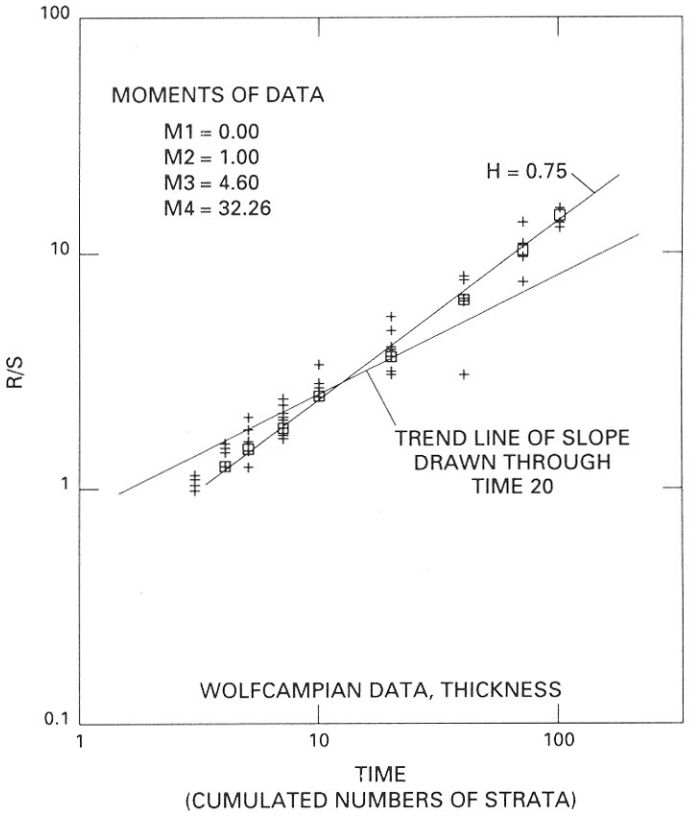


FIGURE 2.16. Pox diagram of $\log R/S$ versus $\log \delta$ for the thickness of bedding during the Wolfcampian era in Kansas, which spanned approximately 21 million years. Data are from a private communication from Dr. G. C. Mann (skewness = 4.60, kurtosis = 32.26; this record is highly non-Gaussian, personal communication). Such records differ from hydrological records in that time is measured in cumulated numbers of strata, where the $n$th item in the record is the thickness of the $n$th stratum.

## REFERENCES

deBeauregard, J., *Electricité de France* (1968).

De Geer, G., *Geochronologia Suecica Principles* (Almquest and Wiksells, Stockholm, 1940).

Eberlein, X. and Taqqu, M. S., *Dependence in Probability and Statistics* (Birkhauser, Boston, 1986).

Feder, J., *Fractals* (Plenum Press, New York, 1988).

Granger, C. W. J. and Hatanaka, M., *Spectral Analysis of Economic Time Series* (Princeton University Press, Princeton, 1964).

Hurst, H. E., *Trans. Am. Soc. Civ. Eng.* **116**, 770 (1951).

———, *Proc. Inst. Civ. Eng.*, 519 (1956).

Hurst, H. E., Black, R. P. and Simaika, Y. M., *Long-Term Storage, an Experimental Study* (Constable, London, 1965).

Langbein, W. B., Contribution to the discussion of Hurst, *Proc. Inst. Civ. Eng.*, 565 (1956).

Mandelbrot, B., *J. Polit. Econ.* **71**, 421 (1963).

Mandelbrot, B., *Comptes-rendus de l'Académie des Sciences (Paris)* **260**, 3274 (1965).

———, *Science* **155**, 636 (1967a).

———, *Encyclopédie de la Pléiade*, Logique et Connaissance Scientifique (J. Piaget, ed.) (Gallimard, Paris, 1967b).
———, *Water Resour. Res.* **7**, 543 (1971).
———, *Zeit Wahr* **31**, 271 (1975).
———, *The Fractal Geometry of Nature* (W. H. Freeman, New York, 1982).
———, *Multifractals: Noise, Turbulence, and Aggregates* (Springer-Verlag, New York, 1991).
Mandelbrot, B. and Van Ness, J. W. *SIAM Review* **10**, 422 (1968).
Mandelbrot, B. and Wallis J. R., *Water Resour. Res.* **4**, 909 (1968).
———, *Water Resour. Res.* **5** (1969a).
———, *Water Resour. Res.* **5**, 967 (1969b).
Munro, E. H., *Terr. Magn.* **53**, 241 (1948).
Schulman, E., *Dendroclimatic Changes in Semiarid America* (University of Arizona Press, Tucson, 1956).
Taqqu, M., *Water Resour. Res.* **6**, 349 (1970).
Toussoun, O., *Mem. Inst. Egypt* 8–10 (1925).
US Bureau of the Census, *The Statistical History of the United States from Colonial Times to the Present* (Fairfield Publishers, Stanford, 1965).
Willett, H. C., *Weather and Our Food Supply* (Iowa State University, Ames, 1964), p. 123–51.

## NOTATIONS

| | |
|---|---|
| $H$ | Hurst's constant (also called Holder constant); the asymptotic slope of the plot of log $(R/S)$ versus log $\delta$. |
| $K$ | Slope of log $R/S$ versus log $\delta$ using the algorithm suggested by Hurst; this $K$ was used as an estimate of $H$, but ordinarily it underestimates the value of $H - 0.72$. |
| $L(G)$ | Length of a coastline as approximated by a $G$-sided polygon with equal sides and vertices lying on the coastline. |
| $\lambda$ | Arbitrary time boundary separating the domains of applicability of two scientific discipline, both of which study a single set of phenomena but use different time scales. |
| $R(t,\delta)$ | Sample bridge range for lag $\delta$. |
| $\delta$ | Time lag. |
| $S^2(t,\delta)$ | Variance of $\delta$ values of $X(t + 1) \ldots X(t + \delta)$ around their sample average. |
| $t$ | Time |
| $T$ | Total available sample size. |
| $X(t)$ | Record containing $T$ readings uniformly space in time from $t = 1$ to $t = T$. |
| $\int x(t)$ | Equal to $\Sigma_{u=1}^{t} x(u)$. |

## APPENDIX: ABSTRACTS AND ERRATA FOR RELATED PAPERS BY THE SAME AUTHORS

*Notation*: In these errata, the letters L and R stand for left and right column, respectively; line −13 stands for line 13 from the bottom of the column.

*Remark*: In all the papers by Mandelbrot and Wallis, the values of $R/S$ for small lags are incorrect and must be disregarded (Taqqu, 1970). These values were not taken into account; hence the papers' conclusions remain unaffected.

### *Noah, Joseph, and Operational Hydrology (Mandelbrot and Wallis, 1968)*

*Abstract*: By the Noah effect, we designate the observation that extreme precipitation can be very extreme indeed, and by Joseph effect, the finding that a long period of unusual

(high or low) precipitation can be extremely long. Current models of statistical hydrology cannot account for either effect and must be superseded. As a replacement, self-similar models appear very promising. They account particularly well for the remarkable empirical observations of Harold Edwin Hurst. The present paper introduces and summarizes a series of investigations on self-similar operational hydrology.

In the papers that the present work introduces and summarizes, the complex interplay between the random variable $R(\delta)/S(\delta)$, its sample distribution, its expectation, and its variance, is described in detail. Therefore the present work postpones all qualification and handles $R(\delta)/S(\delta)$ quite casually. Depending on the context, the same letters $R(\delta)/S(\delta)$ stand for this random variable itself, its expectation, or a sample estimate.

Errata

p. 911 L, line 12, replace 0.5 by $s^{0.5}$.
p. 913 R, line −13, replace expl $(-|s|/s)$ by $\exp(-|s|/s_2)$.
p. 913R line −11, replace $(1+|s|_2/S_3)^{-2}$ by $(1+|s|/S_3)^{-2}$.
p. 914 L, line −14, replace $\Delta X^*$ by $\Delta X^* =$.
p. 915 L, line −3 replace *l:f* by 1:*f*.
p. 916 L, line 28, replace $C\sqrt{s}$ by $K\sqrt{s}$, with some (positive and finite) constant.
p. 916 L, line −5, replace X(u) by C(u).
p. 916 R line 17, replace C a constant by G a random variable independent of t and $s$.
p. 916 R, line −8, replace by $C_H(s) = Q[(s-1)^{2H} - 2s^{2H} + (s+1)^{2H}]$.
p. 916 R, line −6, replace by $C_H(s) = [2H(2H-1)Q]s^{2H-2}$.
p. 916 R, line −9, replace $s \geqslant$ by $s \geqslant 1$.

*Computer Experiments with Fractional Gaussian Noises (Mandelbrot and Wallis, 1969a)*

*Abstract of Part 1*, Averages and variances: Fractional Gaussian noises are a family of random processes such that the interdependence between values of the process at instants of time very distant from each other is small but nonnegligible. It has been shown by mathematical analysis that such interdependence has precisely the intensity required for a good mathematical model of log run hydrological and geophysical records. This analysis is not illustrated, extended, and made practically usable with the help of computer simulations. In Part 1, we stress the shape of the sample functions and relations between past and future averages.

*Abstract of Part 2*, Rescaled ranges and spectra: Continuing the preceding paper, we report on computer experiments on the rescaled range and the spectrum of fractal Gaussian noise.

*Abstract of Part 3*, Mathematical appendix: The present appendix is devoted to mathematical considerations designed to fill in the innumerable logical gaps left in the preceding paper. Even though most proofs are merely sketched or omitted, the notation remains heavy, and some readers may wish to skip to Formulas 1 and 2, which define Type 1 functions.

Mandelbrot and Van Ness (1968) contains additional mathematical details and references.

Errata

Frieze 8 should follow Friezes 1 to 7 along the tops of succeeding pages.
p. 228 L, line 8, replace [1968a] by [1968].

pl. 233 L, line 6, add = (equal sign) so that it reads $\epsilon(\Delta X^*)^2 = \epsilon(\Delta_H)B^2 = C_H s^{2H}$.
p. 233 R, line 11, read $\sqrt{C_H^H}$.
p. 234 R, line −10, add $\epsilon$ to $\epsilon S^2(t,s) = \epsilon X^2 - \epsilon(s^{-1}\Delta X^*)^2$.
p. 234 R, line −3 erase ⊥.
p. 236 L, replace $(P + F)^{2F}$ by $(P + F)^{2H}$.
p. 239, interchange the figures on this and the next page. The captions do not move.
p. 240, replace this figure by the figure on the last page.
p. 240 R, line 2, add − (minus sign) before the second term of $\Delta_{FP}/S_p$.
p. 240 L, line −1, delete the short paragraph beginning with "A corollary of Studen's result . . ."
p. 241 L, line 5, after the table, erase ⊥.
p. 242 L, line −1, replace $\Sigma_{u+1}^t$ by $\Sigma_{u=1}^t$.
p. 243, caption of Figure 1, line −1, replace (in both places) $0 < u$ by $0 \leqslant u$.
p. 243 R, line −17, replace *the* by *either*.
p. 256 R, line 4, replace | by 1.
p. 263 R, line 5, read "that s > 2 and $1 \leqslant$ . . ."

*Robustness of the Rescaled Range R/S in the Measurement of Non-Cyclic Long-Run Statistical Dependence (Mandelbrot and Wallis, 1969b)*

*Abstract*: The rescaled range $R(t,\delta)/S(t,s)$ is shown by extensive computer simulation to be a very robust statistic for testing the presence of noncyclic long-run statistical dependence and for estimating its intensity. Processes examined in the paper include extraordinarily non-Gaussian processes with huge skewness and/or kurtosis (that is, third and/or fourth moments).

*A Fast Fractional Gaussian Noise Generator (Mandelbrot, 1971)*

*Abstract*: By design, fast fractional Gaussian noises (ffGn) have the following characteristics: The number of operations to generate them is relatively small, the long-run statistical dependence that they exhibit is strong and has the form required for self similar hydrology. Their short-run properties, as expressed by correlations between successive or nearly successive yearly averages, are adjustable (within bounds) and can be fitted to the corresponding short-run properties of records. Extension to the multidimensional (multi-site) case should raise no essential difficulty. Finally, their definition, as sums for Markov–Gauss and other simple processes, fits the intuitive ideas that climate can be visualized as either unpredictably inhomogeneous or ruled by a hierarchy of variable regimes.

Erratum

p. 545 R, replace $\dfrac{1 - P^{-(1-H)}H(2H - 1)}{\Gamma(3 - 2H)}$ by $1 - \dfrac{B^{-(1-H)}H(2H - 1)}{\Gamma(3 - 2H)}$